Am J Transl Res 2025;17(5):4038-4053
www.ajtr.org /ISSN:1943-8141/AJTR0163845

Original Article

Development and evaluation of a predictive model for postoperative recurrence and metastasis in breast cancer using an artificial intelligence ultrasound breast system

Xiuli Cheng, Lili Shen, Xinyu Tang, Fang Ma

Department of Ultrasound Medicine, The Second People's Hospital of Hefei, Hefei 230011, Anhui, China

Received February 11, 2025; Accepted April 25, 2025; Epub May 15, 2025; Published May 30, 2025

Abstract: Objective: To assess the feasibility and efficacy of developing a predictive model for postoperative recurrence and metastasis in breast cancer using the Artificial Intelligence Ultrasound Breast System (AIUBS). Methods: A retrospective study was conducted with 120 breast cancer patients who underwent surgery between January 2022 and December 2023. Patients were divided into two groups based on postoperative outcomes: recurrence/metastasis (n = 58) and non-recurrence/non-metastasis (n = 62). Logistic regression was used to identify independent predictors, and a nomogram model was constructed. Model performance was assessed using Receiver Operating Characteristic curves, calibration curves, and decision curve analysis (DCA). The optimal cutoff value was determined through confusion matrix analysis. Results: Univariate analysis identified lymph node metastasis (OR = 8.17, 95% CI: 3.51-18.99), estrogen receptor (ER) status (OR = 0.46, 95% CI: 0.21-0.99), and human epidermal growth factor receptor 2 status (OR = 5.32, 95% CI: 2.32-12.22) as significant predictors. Multivariate analysis confirmed lymph node metastasis (OR = 8.81, 95% CI: 3.68-21.07) and ER status (OR = 0.39, 95% CI: 0.16-0.94) as independent predictors. The nomogram model demonstrated an Area Under the Curve of 0.77 (95% CI: 0.68-0.85). The optimal cutoff value, derived from confusion matrix analysis, was 0.572, confirming the model's clinical utility. Conclusion: The AIUBS-based predictive model for postoperative recurrence and metastasis in breast cancer demonstrates high predictive accuracy and clinical utility, providing valuable support for personalized treatment and follow-up decisions.

Keywords: Breast cancer, postoperative recurrence metastasis, predictive model, artificial intelligence ultrasound breast system

Introduction

In 2020, approximately 19.3 million new cancer cases were diagnosed worldwide, with female breast cancer accounting for 11.7%, slightly surpassing lung cancer at 11.4%. Breast cancer in women has now become the most commonly diagnosed cancer globally, overtaking lung cancer in terms of incidence [1]. Significant progress has been made in breast cancer treatment, with current therapeutic strategies including surgery, chemotherapy, radiotherapy, targeted therapy, and endocrine therapy. These approaches have led to a cure rate of 80-90% for patients with early-stage disease [2]. However, despite these advances, 20-30% of early-stage breast cancer patients still experience tumor recurrence and metastasis [3, 4]. In patients with recurrent or metastatic disease following surgery, the five-year survival rate drops dramatically to only 10% [5]. Clinical research has shown that the risk of postoperative recurrence and metastasis is closely linked to factors such as the tumor's biological characteristics, lymph node involvement, hormone receptor expression, and the Ki-67 proliferation index [6, 7]. Breast cancer can be classified into various subtypes based on clinical and pathological features, with each subtype exhibiting distinct recurrence, metastasis, and survival patterns [8]. Despite advancements in understanding, accurately predicting postoperative recurrence and metastasis-and developing personalized treat-

https://doi.org/10.62347/MECC4748

ment strategies-remains a major challenge in clinical oncology.

Ultrasonography plays a vital role in breast cancer diagnosis, molecular subtyping, and the evaluation of neoadjuvant chemotherapy efficacy, due to its affordability, convenience, and absence of radiation exposure [9]. While manual ultrasound remains the cornerstone of breast cancer screening, challenges such as a shortage of skilled ultrasound physicians and limited expertise in primary healthcare facilities persist [10]. In recent years, artificial intelligence (AI)-assisted screening devices have become a key development in public health services for chronic disease screening. The Artificial In telligence Ultrasound Breast System (AIUBS), which integrates robotic arms for standardized bilateral scanning, cloud-based image storage, AI-driven lesion annotation, and remote interpretation by senior physicians, offers several advantages, including reproducibility, comprehensive scanning, and operation without a sonographer [11]. Studies have demonstrated that AIUBS enhances diagnostic accuracy for breast cancer and improves postoperative follow-up compared to traditional methods [12, 13]. However, most existing studies have primarily focused on assessing the accuracy and safety of these devices, with a lack of large-scale, systematic research to confirm their effectiveness and reliability across diverse clinical environments. Additionally, integrating AI technology with clinical data to develop multifactorial predictive models, evaluating their generalizability, and enhancing their clinical applicability remain significant challenges in current research.

To address these challenges, this study is the first to integrate AIUBS with traditional clinical pathological features to develop a predictive model for postoperative recurrence and metastasis in breast cancer. Using multivariate logistic regression analysis, we combined clinical variables (such as tumor size, lymph node metastasis, estrogen receptor (ER) status, progesterone receptor (PR) status, human epidermal growth factor receptor 2 (HER2), and Ki-67 proliferation index) with imaging features derived from AIUBS (such as tumor morphology, margins, echo features, and blood flow status). This comprehensive approach enabled us to identify independent risk factors associated with postoperative recurrence and metastasis, culminating in a robust predictive model. We believe this model has the potential to significantly enhance the accuracy of predicting recurrence and metastasis in breast cancer patients, ultimately providing clinicians with more precise tools for follow-up and individualized treatment plans. This, in turn, could improve both the quality of life and long-term survival outcomes for breast cancer patients.

Materials and methods

Study population

This retrospective study included patients who underwent breast cancer surgery at the Second People's Hospital of Hefei between January 2022 and December 2023. Postoperative follow-up data were collected from medical records, ensuring both completeness and reliability. All patient information was anonymized, and informed consent was not required due to the retrospective nature of the study. To ensure statistical rigor, a sample size calculation was performed based on previous studies and the anticipated effect size. For comparison between two groups, we assumed an effect size of 0.5, a significance level of 0.05, and a statistical power of 0.8. Using GPower software, the minimum required sample size was determined to be 120 patients. Accordingly, a total of 120 patients were included, meeting the statistical criteria for analysis.

Patient classification and group division

The patients were classified into two groups based on their recurrence or metastasis status: the recurrence and metastasis group (n = 58) and the non-recurrence and non-metastasis group (n = 62). The inclusion criteria were: 1) patients aged between 18 and 75 years who underwent either radical or breast-conserving surgery for breast cancer; 2) continuous postoperative follow-up in accordance with national treatment guidelines; 3) preoperative pathological diagnosis of breast cancer supported by routine clinical and imaging examinations; and 4) voluntary participation with signed informed consent. The exclusion criteria were: 1) incomplete postoperative treatment or failure to undergo necessary imaging examinations during follow-up; 2) patients with severe systemic diseases, such as heart, liver, or kidney disorders;

3) missing data or poor-quality ultrasound images unsuitable for analysis; and 4) other diseases that could confound the evaluation of breast cancer recurrence and metastasis. This study was approved by the Institutional Review Board (IRB) of the Second People's Hospital of Hefei and adhered to the ethical guidelines outlined in the Declaration of Helsinki.

To evaluate the stability and external validity of the predictive model, the dataset of 120 patients was randomly divided into a training set (96 patients) and a validation set (24 patients), with an 80% to 20% ratio. The distribution of key clinical variables, including gender, age, tumor stage, and lymph node metastasis, was balanced between the two sets to ensure comparability in patient characteristics. Furthermore, the model's external validity was further tested using an external validation cohort from another hospital, with data collected between January 2022 and December 2023. This cohort included 50 patients with recurrence and metastasis and 55 patients without recurrence or metastasis. The inclusion criteria and screening procedures for the external cohort were consistent with those applied in the original study.

Clinical and ultrasound imaging data collection

Basic clinical data, including age, weight, tumor size, lymph node metastasis status, tumor stage (TNM), hormone receptor status (ER, PR), HER2, and Ki-67 proliferation index, were collected. These data were extracted from the patients' electronic medical records by trained researchers to ensure accuracy and consistency.

Post-treatment ultrasound data were retrospectively obtained from medical records and analyzed using the Samsung RS80A ultrasound system integrated with the AIUBS module. This AIUBS system facilitated the automated extraction of both quantitative (e.g., maximum diameter) and qualitative (e.g., shape [round, oval, irregular], margins [smooth, spiculated], echogenicity [homogeneous, heterogeneous], and blood flow [present/absent]) tumor features from ultrasound images. To ensure quality and minimize the influence of artifacts, rigorous quality control protocols were applied during ultrasound examinations, including the use of standardized denoising algorithms. Furthermore, all ultrasound images were independently reviewed by two experienced radiologists to ensure data reliability and inter-observer consistency.

Data analysis with AIUBS

The Samsung RS80A ultrasound system, integrated with AIUBS, automatically detects and annotates tumors in ultrasound images while extracting multiple image features. Using deep learning algorithms, the AIUBS system identifies key characteristics of breast tumors, such as size, shape, margin properties, echogenicity patterns, and blood flow. Each feature is automatically labeled and quantified by the AI system, which then processes the data using a pre-trained model. The results from the AIUBS system were used as essential input features for constructing the recurrence and metastasis prediction model, in combination with clinical data.

Statistical analysis

All statistical analyses were performed using R software (version 4.0.3; R Foundation for Statistical Computing, Vienna, Austria). All statistical tests were two-sided, with a significance level predetermined at $P < 0.05$.

Data description and testing: Continuous variables are presented as mean ± standard deviation (SD) or median (interquartile range, IQR), depending on the distribution's normality. Group comparisons for continuous variables were performed using Student's t-test or the Mann-Whitney U test, as appropriate. Categorical variables are presented as frequencies and percentages, with intergroup differences assessed using the chi-square test.

Data preprocessing and model construction: Multivariable logistic regression analysis, conducted using the 'glm' package in R, was employed to identify independent predictors of post-surgical recurrence and metastasis in breast cancer. This model evaluated the independent associations between clinical variables (e.g., tumor size, hormone receptor status, and lymph node metastasis) and recurrence/metastasis. Regression coefficients, along with their corresponding 95% confidence intervals (CIs), were calculated to quantify the effect size of each predictor. The threshold for

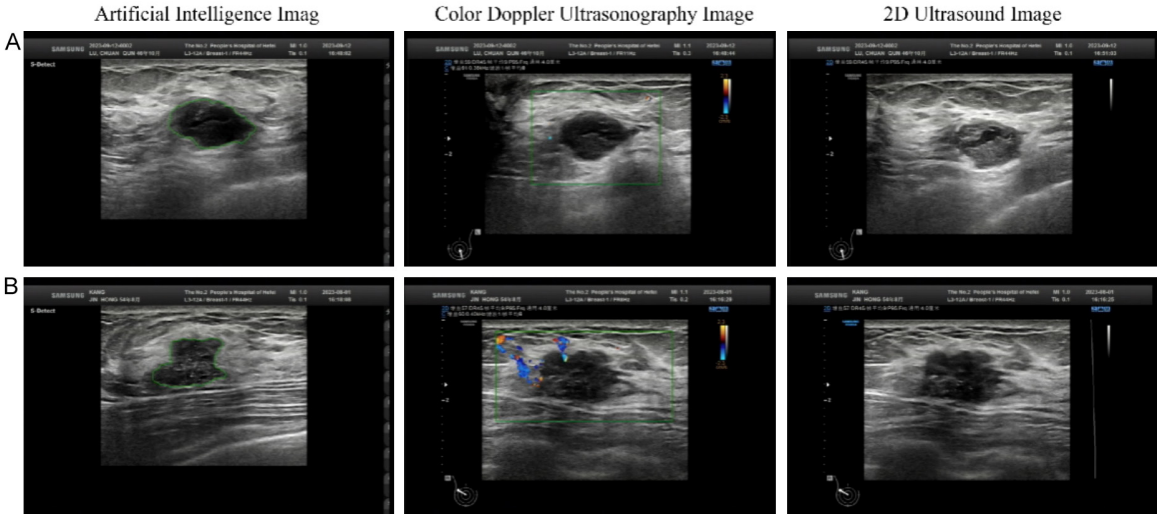

Figure 1. Ultrasound images of typical cases. A: Non-recurrence and non-metastasis group. Left breast invasive carcinoma, grade II, invasive ductal carcinoma (IDC), not otherwise specified (NOS) (tumor size: 1.5 cm × 1.5 cm × 1.2 cm). The image shows the presence of the nipple and solid structure, with abundant stromal lymphocytic infiltration. B: Recurrence and metastasis group. Right breast invasive carcinoma, grade II, IDC-NOS (tumor size: 2.3 cm × 2.0 cm × 1.5 cm). A focal region displays moderate to high-grade ductal carcinoma in situ (DCIS) with central necrosis and calcification. No clear evidence of lymphovascular invasion or nerve involvement is observed.

statistical significance was set at $P < 0.05$. Stepwise variable selection, guided by either the Akaike Information Criterion (AIC) or the Bayesian Information Criterion (BIC), was employed to optimize model fit and parsimony. Non-significant variables were then excluded from the final model. To ensure robust model evaluation and assess generalizability, the dataset was randomly divided into a training set (80%, n = 96) and a validation set (20%, n = 24). Stratified random sampling was used to ensure a uniform distribution of key clinical factors (e.g., age, tumor stage, and lymph node status) across both sets. The training set was used for model development and parameter estimation, while the validation set served as an independent benchmark for model performance.

Model evaluation: The model's predictive performance was evaluated using receiver operating characteristic (ROC) curve analysis, with the area under the ROC curve (AUC) quantified using the 'pROC' package in R. Data visualization, including calibration curves and decision curves, was implemented using the 'ggplot2' package. The AUC, ranging from 0.5 (representing random chance) to 1.0 (indicating perfect discrimination), quantifies the model's discriminatory capacity between patients with and without recurrence or metastasis. Model calibration was assessed using calibration curves, which compare predicted probabilities with observed outcomes. A well-calibrated model shows strong agreement between predicted and observed probabilities, reflected by proximity to the diagonal line.

Decision curve analysis (DCA) was performed to evaluate the clinical utility of the model by quantifying the net benefit across a range of threshold probabilities. DCA provides insights into the potential impact of the model on clinical decision-making and helps determine whether its implementation results in better patient outcomes compared to "treat-all" or "treat-none" approaches.

Results

Comparison of patient characteristics

This study included 120 patients, with 58 (48.33%) assigned to the recurrence/metastasis group and 62 (51.67%) to the non-recurrence/non-metastasis group. Regarding ultrasound imaging findings, the non-recurrence/non-metastasis group (**Figure 1A**) showed an invasive ductal carcinoma (IDC) of the left breast, grade II, not otherwise specified (NOS),

with a tumor size of 1.5 cm × 1.5 cm × 1.2 cm. The image revealed a solid structure adjacent to the nipple with abundant stromal lymphocytic infiltration, well-defined margins, and homogeneous internal echoes. In contrast, the recurrence/metastasis group (**Figure 1B**) displayed an invasive carcinoma of the right breast, grade II, IDC-NOS, with a tumor size of 2.3 cm × 2.0 cm × 1.5 cm. The ultrasound image revealed irregular morphology, ill-defined borders, and heterogeneous internal echoes. Focal areas exhibited moderate to high-grade ductal carcinoma in situ (DCIS) with central necrosis and calcification, suggesting higher malignant potential. No obvious evidence of lymphovascular invasion or perineural involvement was observed.

No significant age difference was observed between the two groups (P = 0.702) (**Table 1**). Regarding tumor characteristics, the recurrence/metastasis group had significantly larger tumor size, higher Ki-67 index, more pronounced ultrasound blood flow, higher AIUBS strain ratio, and higher gray-scale mean values compared to the non-recurrence/non-metastasis group (all P < 0.05). Significant differences were also observed for tumor stage and lymph node metastasis (both P < 0.001). The recurrence/metastasis group predominantly presented with Stage II tumors but exhibited a reduced incidence of lymph node metastasis. Additionally, the recurrence/metastasis group showed significant differences in ultrasound morphology, texture features, and HER2 status compared to the non-recurrence/non-metastasis group (all P < 0.05). Tumor size, Ki-67 expression, ultrasound features, lymph node metastasis, and HER2 status were all correlated with tumor recurrence and metastasis.

Selection of predictive factors and nomogram model construction

Univariate logistic regression analysis identified several potential predictive factors for postoperative recurrence and metastasis in breast cancer (**Table 2**). Lymph node metastasis [Odds Ratio (OR) = 8.17, 95% Confidence Interval (CI): 3.51-18.99], ER status (OR = 0.46, 95% CI: 0.21-0.99), and HER2 status (OR = 5.32, 95% CI: 2.32-12.22) exhibited statistical significance, with the ORs highlighting the predictive importance of these factors in recurrence and metastasis.

Multivariate logistic regression analysis confirmed the independent predictive value of lymph node metastasis (OR = 8.81, 95% CI: 3.68-21.07) and ER status (OR = 0.39, 95% CI: 0.16-0.94) (**Table 3**). The OR for lymph node metastasis was significantly greater than 1, indicating a strong association with the risk of recurrence and metastasis. Conversely, the OR for ER status was less than 1, suggesting that ER-positive status may be associated with a reduced risk of recurrence and metastasis. The final model for predicting postoperative recurrence and metastasis in breast cancer is as follows: $\log\frac{P}{1-P} = \beta_0 + \beta_1 \times \text{LNM} + \beta_2 \times \text{ER}$

Where:

P is the probability of post-surgical recurrence and metastasis in breast cancer.

β_0 is the intercept, which equals -0.29.

Lymph Node Metastasis (LNM): 0 = no, 1 = yes, with a regression coefficient $\beta_1 = 2.18$.

ER status: 0 = negative, 1 = positive, with a regression coefficient $\beta_2 = -0.95$.

A nomogram was constructed based on these independent predictors to estimate the risk of postoperative recurrence and metastasis (**Figure 2**). The nomogram assigns points to each factor, which are then summed to obtain a total score corresponding to the predicted probability of recurrence/metastasis. This model provides a convenient tool for clinical risk assessment and aids in the accurate prediction of postoperative prognosis for breast cancer patients.

Model performance evaluation

The predictive model, constructed using the independent risk factors identified earlier, exhibited favorable discriminatory performance, with an AUC of 0.77 (95% CI: 0.68-0.85) (**Figure 3A**). Calibration curves for both the training and validation cohorts demonstrated strong agreement with the ideal diagonal, confirming the model's robust calibration and generalizability (**Figure 3B**). DCA demonstrated a substantial

Table 1. Basic characteristics and differential analysis

Variables	Total (n = 120)	Recurrence_and_Metastasis_Group (n = 58)	Non_Recurrence_and_Non Metastasis_Group (n = 62)	Statistic	*P*
Age, Mean ± SD	49.72 ± 8.27	50.02 ± 8.73	49.44 ± 7.89	T = 0.38	0.702
Tumor Size (cm), M (Q_1, Q_3)	2.80 (2.10, 3.70)	3.35 (2.32, 4.65)	2.60 (2.00, 3.18)	Z =- 3.38	< 0.001
Ki 67(%), M (Q_1, Q_3)	26.00 (19.75, 36.25)	37.00 (27.00, 50.00)	20.50 (15.00, 25.75)	Z = -6.72	< 0.001
Ultrasound Feature Blood Flow, M (Q_1, Q_3)	4.00 (2.00, 5.00)	4.00 (4.00, 5.00)	3.00 (1.00, 5.00)	Z = -3.11	0.002
AIUBS Analysis Strain Ratio, M (Q_1, Q_3)	3.50 (2.77, 4.40)	4.75 (3.32, 6.18)	3.25 (2.50, 3.60)	Z = -5.14	< 0.001
AIUBS Analysis Gray Mean Value, M (Q_1, Q_3)	59.00 (51.00, 66.25)	51.00 (44.25, 58.75)	64.00 (59.00, 68.00)	Z = -5.58	< 0.001
Stage, n (%)				-	< 0.001
I	31 (25.83)	21 (33.87)	10 (17.24)		
II	54 (45.00)	36 (58.06)	18 (31.03)		
III	28 (23.33)	5 (8.06)	23 (39.66)		
IV	7 (5.83)	0 (0.00)	7 (12.07)		
Ultrasound Feature Boundary, n (%)				-	0.061
Blurred	59 (49.17)	33 (53.23)	26 (44.83)		
Clear	56 (46.67)	29 (46.77)	27 (46.55)		
Relatively_Clear	5 (4.17)	0 (0.00)	5 (8.62)		
Ultrasound Feature Morphology, n (%)				-	< 0.001
Circular	6 (5.00)	0 (0.00)	6 (10.34)		
Irregular	54 (45.00)	20 (32.26)	34 (58.62)		
Oval	12 (10.00)	0 (0.00)	12 (20.69)		
Regular	42 (35.00)	42 (67.74)	0 (0.00)		
Relatively_regular	6 (5.00)	0 (0.00)	6 (10.34)		
AIUBS Analysis Texture, n (%)				-	< 0.001
Blurred	7 (5.83)	0 (0.00)	7 (12.07)		
Rough	29 (24.17)	0 (0.00)	29 (50.00)		
Sharp	4 (3.33)	4 (6.45)	0 (0.00)		
Smooth	80 (66.67)	58 (93.55)	22 (37.93)		
LNM, n (%)				χ^2 = 26.48	< 0.001
No	72 (60.00)	51 (82.26)	21 (36.21)		
Yes	48 (40.00)	11 (17.74)	37 (63.79)		
ER Status, n (%)				χ^2 = 3.99	0.046
Negative	41 (34.17)	16 (25.81)	25 (43.10)		
Positive	79 (65.83)	46 (74.19)	33 (56.90)		

PR Status, n (%)				$\chi^2 = 0.03$	0.869
Negative	57 (47.50)	29 (46.77)	28 (48.28)		
Positive	63 (52.50)	33 (53.23)	30 (51.72)		
HER2 Status, n (%)				$\chi^2 = 16.79$	< 0.001
Negative	78 (65.00)	51 (82.26)	27 (46.55)		
Positive	42 (35.00)	11 (17.74)	31 (53.45)		
AIUBS Analysis Elasticity Score, n (%)				$\chi^2 = 7.59$	0.108
1	5 (4.17)	0 (0.00)	5 (8.62)		
2	26 (21.67)	16 (25.81)	10 (17.24)		
3	26 (21.67)	13 (20.97)	13 (22.41)		
4	36 (30.00)	21 (33.87)	15 (25.86)		
5	27 (22.50)	12 (19.35)	15 (25.86)		

t: t-test, Z: Mann-Whitney test, χ^2: Chi-square test, -: Fisher exact, SD: standard deviation, M: Median, Q_1: 1st Quartile, Q_3: 3st Quartile, AIUBS: Artificial Intelligence Ultrasound Breast System, LNM: Lymph Node Metastasis, ER: estrogen receptor, PR: progesterone receptor, HER2: human epidermal growth factor receptor 2.

Table 2. Univariate logistic regression analysis

Variables	β	S.E	Z	*P*	OR (95% CI)
Ultrasound Feature Boundary					
Blurred					1.00 (Reference)
Clear	0.17	0.37	0.45	0.656	1.18 (0.57 - 2.46)
Relatively_Clear	16.80	1073.11	0.02	0.988	19865188.69 (0.00 - Inf)
Stage					
I					1.00 (Reference)
II	0.05	0.48	0.10	0.919	1.05 (0.41 - 2.69)
III	2.27	0.63	3.63	< 0.001	9.66 (2.84 - 32.91)
IV	18.31	1495.30	0.01	0.990	89344105.92 (0.00 - Inf)
AIUBS Analysis Texture					
Blurred					1.00 (Reference)
Rough	-0.00	4528.70	-0.00	1.000	1.00 (0.00 - Inf)
Sharp	-39.13	6740.43	-0.01	0.995	0.00 (0.00 - Inf)
Smooth	-20.54	4064.63	-0.01	0.996	0.00 (0.00 - Inf)
LNM					
No					1.00 (Reference)
Yes	2.10	0.43	4.88	< 0.001	8.17 (3.51 - 18.99)
Ultrasound Feature Morphology					
Circular					1.00 (Reference)
Irregular	-20.04	7238.39	-0.00	0.998	0.00 (0.00 - Inf)
Oval	-0.00	8865.19	-0.00	1.000	1.00 (0.00 - Inf)
Regular	-41.13	7738.17	-0.01	0.996	0.00 (0.00 - Inf)
Relatively_regular	-0.00	10236.63	-0.00	1.000	1.00 (0.00 - Inf)
ER Status					
negative					1.00 (Reference)
Positive	-0.78	0.39	-1.98	0.048	0.46 (0.21 - 0.99)
PR Status					
negative					1.00 (Reference)
Positive	-0.06	0.37	-0.16	0.869	0.94 (0.46 - 1.93)
HER2 Status					
negative					1.00 (Reference)
Positive	1.67	0.42	3.94	< 0.001	5.32 (2.32 - 12.22)
AIUBS Analysis Elasticity Score					
1					1.00 (Reference)
2	-17.04	1073.11	-0.02	0.987	0.00 (0.00 - Inf)
3	-16.57	1073.11	-0.02	0.988	0.00 (0.00 - Inf)
4	-16.90	1073.11	-0.02	0.987	0.00 (0.00 - Inf)
5	-16.34	1073.11	-0.02	0.988	0.00 (0.00 - Inf)

β: Beta coefficient, S.E.: Standard Error, Z: Z-score, P: *P*-value, OR: Odds Ratio, CI: Confidence Interval, AIUBS: Artificial Intelligence Ultrasound Breast System, LNM: Lymph Node Metastasis, ER: estrogen receptor, PR: progesterone receptor, HER2: human epidermal growth factor receptor 2.

net benefit across a range of threshold probabilities (10%-60%) (**Figure 4**). This suggests that integrating the model into clinical decision-making could improve patient outcomes by enabling more personalized treatment strategies, particularly for patients at elevated risk.

Determination of the optimal cutoff value for the nomogram

To determine the optimal cutoff value for the nomogram, confusion matrix analysis was performed. At a cutoff value of 0.572, the model

Table 3. Multivariate logistic regression analysis

Variables	β	S.E	Z	*P*	OR (95% CI)
Intercept	-0.29	0.37	-0.79	0.432	0.75 (0.36 - 1.55)
LNM					
No					1.00 (Reference)
Yes	2.18	0.45	4.89	< 0.001	8.81 (3.68 - 21.07)
ER Status					
negative					1.00 (Reference)
Positive	-0.95	0.45	-2.11	0.035	0.39 (0.16 - 0.94)

β: Beta coefficient, S.E.: Standard Error, Z: Z-score, P: *P*-value, OR: Odds Ratio, CI: Confidence Interval, LNM: Lymph Node Metastasis, ER: estrogen receptor.

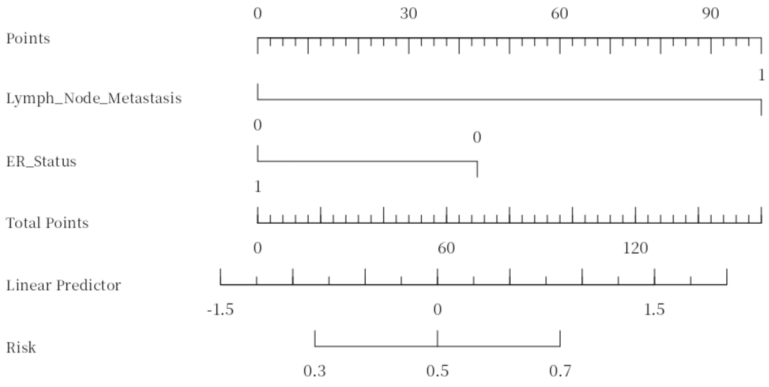

Figure 2. Nomogram for predicting postoperative recurrence and metastasis risk in breast cancer. The total points are obtained by adding the points for each feature, and the corresponding "recurrence risk" is determined by drawing a vertical line from the total points. ER: estrogen receptor.

achieved an accuracy of 0.27 (95% CI: 0.19-0.36), sensitivity of 0.36 (95% CI: 0.24-0.89), specificity of 0.18 (95% CI: 0.08-0.27), positive predictive value (PPV) of 0.29 (95% CI: 0.19-0.40), and negative predictive value (NPV) of 0.23 (95% CI: 0.11-0.35) (**Table 4**). While these metrics suggest some clinical applicability, they also highlight the need for further improvements to enhance the model's accuracy and specificity at this particular cutoff.

External validation and model robustness evaluation

Baseline characteristics of the external datasets are summarized in **Table 5**. To assess the generalizability of the proposed model, its performance was evaluated using an independent external dataset. ROC curve analysis indicated that the model achieved an AUC of 0.79 (95% CI: 0.73-0.85) on the external validation set (**Figure 5A**), showing strong discrimination capability for new data, which is comparable to the AUC of 0.77 from the training set, and even slightly higher. Additionally, the calibration curve (**Figure 5B**) demonstrated high consistency between the model's predicted probability of recurrence and metastasis and the actual observed incidence, further supporting the model's reliability.

Confusion matrix analysis (**Figure 5C**) further confirmed the model's classification performance. The calculated sensitivity, specificity, PPV, and NPV suggest that the model effectively distinguishes between high-risk and low-risk patients, emphasizing its clinical applicability. However, some misclassifications were observed, indicating that the model should be used in conjunction with other clinical factors for comprehensive decision-making in certain clinical scenarios. DCA (**Figure 5D**) revealed that the model consistently provides higher net benefits across a range of high-risk threshold probabilities, particularly within the 0.2-0.6 threshold range, where the clinical benefit of the model significantly exceeds the strategies of "treat all" or "treat none". This further supports the model's potential for clinical application.

Discussion

Conventional approaches to predicting postoperative recurrence and metastasis in breast cancer primarily rely on clinicopathological factors, including tumor size, lymph node metastasis, molecular markers (e.g., ER, PR, HER2), and pathological staging. While these factors provide valuable prognostic information, their predictive accuracy remains limited. As a result, the development of novel and more accurate prediction methods is a critical area of focus in breast cancer research. In recent years, AIUBS, which uses deep learning algorithms to analyze ultrasound imaging data, has emerged as a promising tool. AIUBS offers quantifiable imaging biomarkers that can refine the prediction of

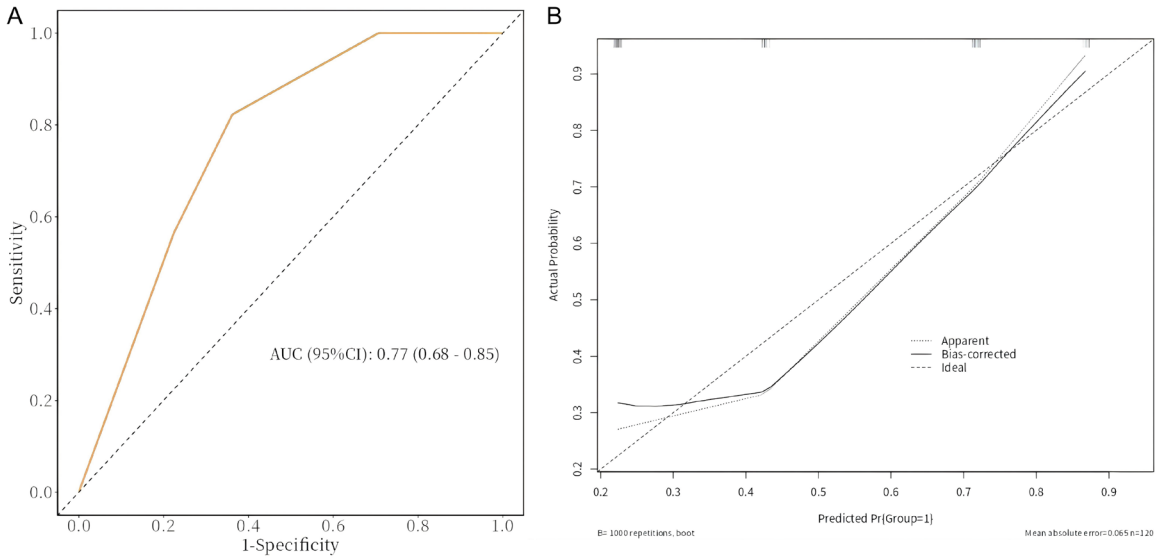

Figure 3. Model performance evaluation. A: Receiver Operating Characteristic (ROC) Curve. B: Calibration Curve. AUC: Area Under the Curve.

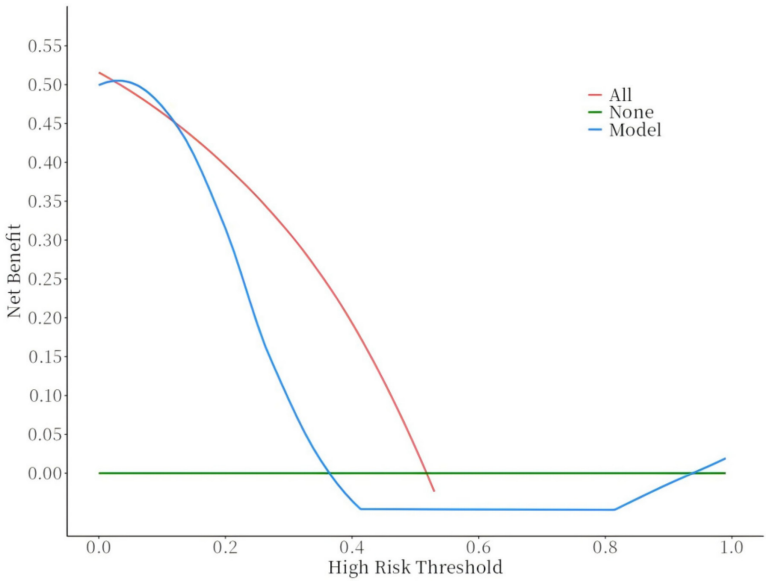

Figure 4. Decision curve analysis (DCA).

tumor aggressiveness and metastatic potential [14]. By quantifying tumor echotexture, morphological irregularity, and vascularity, AIUBS enables a more detailed characterization of tumors. These imaging biomarkers not only reflect tumor biology but also provide insights into the tumor's invasive behavior and metastatic potential [12, 15]. In patients with tumors displaying morphological irregularities, AIUBS offers a complementary approach for early prediction of recurrence and metastasis, especially when conventional imaging techniques face limitations in detecting subtle lesions due to its enhanced resolution and sensitivity.

Our analysis of data from 120 breast cancer patients identified several independent predictors significantly associated with postoperative recurrence and metastasis. Both univariate and multivariate logistic regression analyses identified lymph node metastasis, ER status, and HER2 status as independent risk factors. Lymph node metastasis, which indicates local tumor spread and inherent tumor aggressiveness, is a well-recognized adverse prognostic factor. Its inclusion in the American Joint Committee on Cancer staging criteria, along with its frequent correlation with advanced disease stages and poorer survival outcomes [16], further highlights its clinical significance. Current clinical guidelines for breast cancer recognize lymph node status as a crucial determinant of treatment strategy and prognosis [17]. Therefore, the presence of lymph node metastasis underscores an increased risk of recurrence and metastasis,

Table 4. Confusion matrix for the nomogram model

AUC (95% CI)	Accuracy (95% CI)	Sensitivity (95% CI)	Specificity (95% CI)	PPV (95% CI)	NPV (95% CI)	cut off
0.77 (0.68-0.85)	0.27 (0.19-0.36)	0.36 (0.24 - 0.89)	0.18 (0.08 - 0.27)	0.29 (0.19 - 0.40)	0.23 (0.11 - 0.35)	0.572

AUC: Area Under the Curve, PPV: positive predictive value, NPV: negative predictive value.

reinforcing its pivotal role in breast cancer management. In contrast, ER-positive breast cancer is generally associated with a lower recurrence risk, which is consistent with our finding that ER-positive status serves as a biomarker for reduced recurrence risk [18]. Furthermore, HER2-positive breast cancer is frequently associated with a higher risk of recurrence and distant metastasis, emphasizing the importance of HER2 status in clinical decisions related to recurrence risk assessment and targeted therapy selection [19].

Multivariate regression analysis confirmed the independent predictive significance of lymph node metastasis and ER status, demonstrating their substantial clinical relevance. The elevated odds ratio for lymph node metastasis (OR = 8.81, 95% CI: 3.68-21.07) highlights its strong association with an increased risk of recurrence, while the lower odds ratio for ER-positive status (OR = 0.39, 95% CI: 0.16-0.94) suggests a relatively reduced recurrence risk in ER-positive patients. This finding aligns with the established role of molecular subtypes in breast cancer prognosis. Using these independent risk factors, we developed a nomogram model to predict postoperative recurrence and metastasis. This model provides clinicians with a practical tool for evaluating individual patient risk profiles, facilitating the integration of objective data with clinical expertise to create more personalized treatment strategies. While the Ki-67 proliferation index and hormone receptor status (ER-negative, PR-negative) are acknowledged as relevant factors in breast cancer, their predictive value was not substantiated in our final multivariate model. Existing literature suggests that elevated Ki-67 expression indicates accelerated tumor cell proliferation and increased invasiveness, implying a higher recurrence risk [20, 21]. Additionally, ER-negative and PR-negative tumors, typically indicative of hormone receptor-negative breast cancer, are often associated with a less favorable prognosis and reduced responsiveness to endocrine therapy, contributing to an increased recurrence risk [22, 23].

AIUBS utilizes 3D volumetric imaging, offering a novel modality for breast assessment. This technique provides multiplanar visualization of the breast, including sagittal, transverse, and reconstructed coronal plane images, thereby enhancing lesion margin conspicuity and aiding in the differentiation between benign and malignant entities [24]. AIUBS has been widely applied in breast cancer screening, tumor characterization, and evaluating response to neoadjuvant chemotherapy [25]. Clinical investigations have indicated that AIUBS can improve breast cancer detection rates. For example, Giger et al. [26] reported a 23.9% increase in sensitivity for detecting mammography-negative cancers and a 5.9% increase for mammography-positive cancers, while maintaining comparable false-positive rates. Similarly, Jeh et al. [27], in evaluating 206 lesions across 173 patients using AIUBS, reported a sensitivity of 88.05% and a specificity of 76.25% for differentiating between benign and malignant lesions. However, research on the use of AIUBS for detecting postoperative recurrence and metastasis in breast cancer remains limited. In the present study, the integration of artificial intelligence algorithms wi th ultrasound breast system significantly enhanced the predictive performance for postoperative recurrence and metastasis, demonstrating robust stability across diverse datasets.

Other studies have highlighted the potential of AI-based non-invasive methods for assessing lymph node metastasis and improving the prediction of lymph node involvement [28]. For instance, Sun et al. [29] employed convolutional neural networks (CNNs) to predict axillary lymph node metastasis from primary breast cancer ultrasound images, reporting an AUC of 0.72, an accuracy of 72.6%, a sensitivity of 65.5%, and a specificity of 78.9%. Similarly, Gu et al. [30] developed two deep learning nomograms that integrated ultrasound images and clinical features from a cohort of 484 breast cancer patients before and after neoadjuvant chemotherapy (NAC). These nomograms demonstrated robust predictive performance for

Table 5. Basic characteristics and differential analysis of external data sets

Variables	Total (n = 105)	Recurrence and Metastasis Group (n = 50)	Non-Recurrence and Non-Metastasis Group (n = 55)	Statistic	*P*
Age, Mean ± SD	49.55 ± 8.15	50.60 ± 8.55	48.95 ± 7.80	t = 0.40	0.689
Tumor Size (cm), M (Q_1, Q_3)	2.85 (2.12, 3.80)	3.40 (2.40, 4.50)	2.65 (2.00, 3.25)	Z = -3.25	< 0.001
Ki 67(%), M (Q_1, Q_3)	26.50 (20.00, 37.00)	38.00 (28.00, 51.00)	21.00 (15.50, 26.00)	Z = -6.50	< 0.001
Ultrasound Feature Blood Flow, M (Q_1, Q_3)	4.00 (2.00, 5.00)	4.00 (3.50, 5.00)	3.00 (1.50, 5.00)	Z = -3.00	0.003
AIUBS Analysis Strain Ratio, M (Q_1, Q_3)	3.45 (2.80, 4.35)	4.65 (3.25, 6.10)	3.30 (2.50, 3.75)	Z = -5.00	< 0.001
AIUBS Analysis Gray Mean Value, M (Q_1, Q_3)	58.50 (50.50, 65.75)	50.80 (44.00, 58.20)	63.80 (58.80, 67.80)	Z = -5.40	< 0.001
Stage, n (%)				-	< 0.001
I	27 (25.71)	18 (36.00)	9 (16.36)		
II	46 (43.81)	29 (58.00)	17 (30.91)		
III	26 (24.76)	3 (6.00)	23 (41.82)		
IV	6 (5.71)	0 (0.00)	6 (10.91)		
Ultrasound Feature Boundary, n (%)				-	0.064
Blurred	50 (47.62)	27 (54.00)	23 (41.82)		
Clear	49 (46.67)	23 (46.00)	26 (47.27)		
Relatively_Clear	6 (5.71)	0 (0.00)	6 (10.91)		
Ultrasound Feature Morphology, n (%)				-	< 0.001
Circular	5 (4.76)	0 (0.00)	5 (9.09)		
Irregular	46 (43.81)	14 (28.00)	32 (58.18)		
Oval	10 (9.52)	0 (0.00)	10 (18.18)		
Regular	38 (36.19)	36 (72.00)	2 (3.64)		
Relatively_regular	6 (5.71)	0 (0.00)	6 (10.91)		
AIUBS Analysis Texture, n (%)				-	< 0.001
Blurred	6 (5.71)	0 (0.00)	6 (10.91)		
Rough	24 (22.86)	0 (0.00)	24 (43.64)		
Sharp	4 (3.81)	4 (8.00)	0 (0.00)		
Smooth	71 (67.62)	46 (92.00)	25 (45.45)		
LNM, n (%)				χ^2 = 25.10	< 0.001
No	63 (60.00)	42 (84.00)	21 (38.18)		
Yes	42 (40.00)	8 (16.00)	34 (61.82)		
ER Status, n (%)				χ^2 = 3.76	0.052
Negative	35 (33.33)	12 (24.00)	23 (41.82)		
Positive	70 (66.67)	38 (76.00)	32 (58.18)		

PR Status, n (%)				χ^2 = 0.05	0.829
Negative	51 (48.57)	24 (48.00)	27 (49.09)		
Positive	54 (51.43)	26 (52.00)	28 (50.91)		
HER2 Status, n (%)				χ^2 = 15.80	< 0.001
Negative	68 (64.76)	42 (84.00)	26 (47.27)		
Positive	37 (35.24)	8 (16.00)	29 (52.73)		
AIUBS Analysis Elasticity Score, n (%)				χ^2 = 7.10	0.115
1	4 (3.81)	0 (0.00)	4 (7.27)		
2	22 (20.95)	14 (28.00)	8 (14.55)		
3	22 (20.95)	11 (22.00)	11 (20.00)		
4	32 (30.48)	18 (36.00)	14 (25.45)		
5	25 (23.81)	7 (14.00)	18 (32.73)		

t: t-test, Z: Mann-Whitney test, χ^2: Chi-square test, -: Fisher exact, SD: standard deviation, M: Median, Q_1: 1st Quartile, Q_3: 3st Quartile, AIUBS: Artificial Intelligence Ultrasound Breast System, LNM: Lymph Node Metastasis, ER: estrogen receptor, PR: progesterone receptor, HER2: human epidermal growth factor receptor 2.

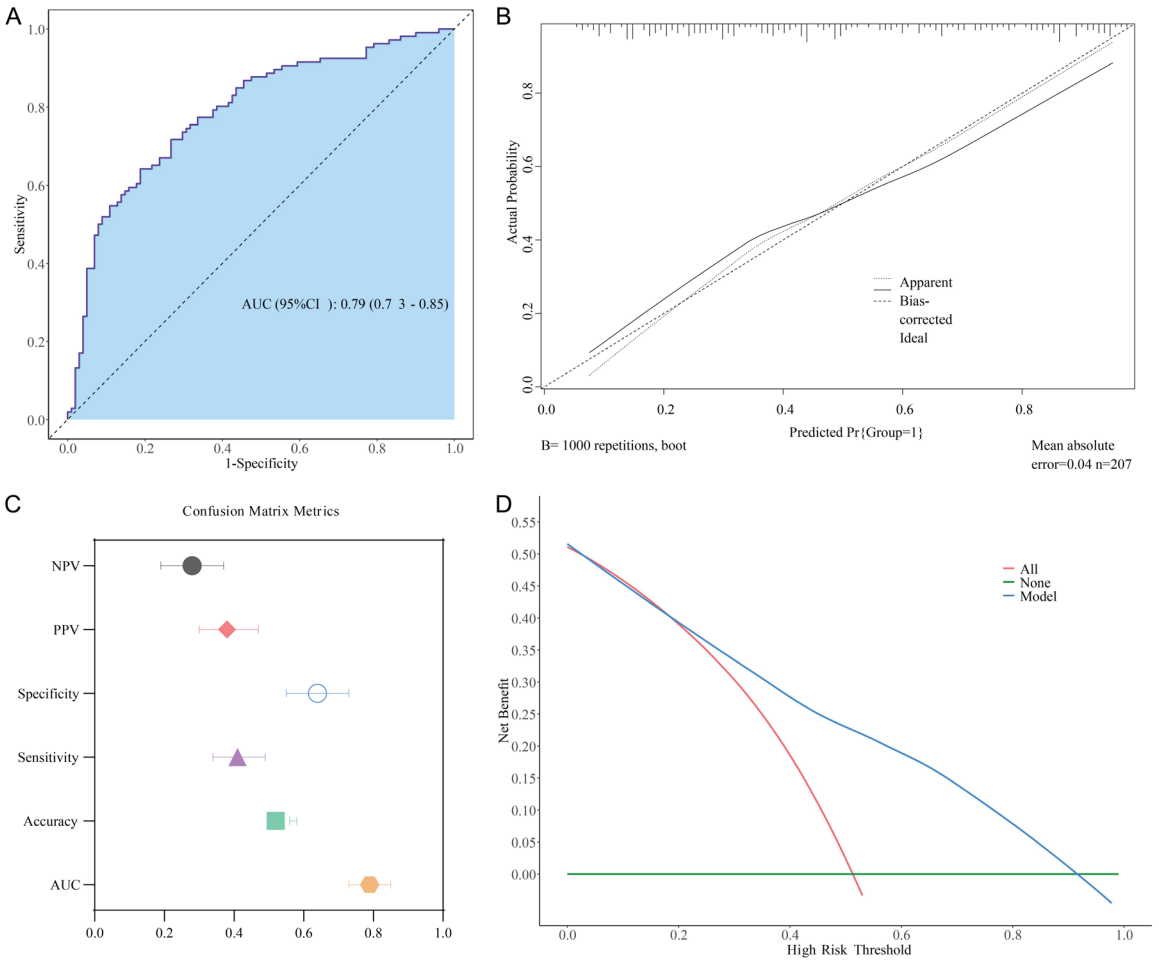

Figure 5. Performance of the model on external data sets. A: Receiver operating characteristic (ROC) curve of the model in the external dataset. B: Calibration curve illustrates the agreement between the model's predicted probabilities and the actual clinical outcomes. C: Confusion matrix metrics of the model in the external dataset. D: Decision curve analysis (DCA) displaying the net benefit of the model at various risk thresholds. AUC: Area Under the Curve. NPV: Negative Predictive Value, PPV: Positive Predictive Value.

tumor response to NAC, with AUCs of 0.903 and 0.896, respectively, and for post-chemotherapy axillary lymph node status, with AUCs of 0.853 and 0.863 in independent validation and test sets. In alignment with these reports, our AI-ABUS-based model achieved an AUC of 0.77, demonstrating compelling predictive capability and satisfactory generalizability. The calibration curve exhibited close proximity to the ideal diagonal, indicating favorable concordance between predicted and observed outcomes. Moreover, DCA revealed that the model significantly enhanced the net benefit of clinical decision-making across a clinically relevant risk threshold range of 10%-60%.

Compared to traditional clinicopathological features, AIUBS provides quantitative imaging characteristics with enhanced sensitivity and accuracy, particularly for detecting small lesions. The invasive potential of breast cancer cells is intrinsically linked to angiogenesis and lymphangiogenesis, processes that promote tumor dissemination and metastasis through modulation of the tumor microenvironment [31]. With its high-resolution imaging capabilities, AIUBS can capture subtle structural changes associated with these processes, providing more refined insights into predicting breast cancer recurrence and metastasis.

This study does have certain limitations. First, the relatively small sample size warrants validation of the model's stability and generalizability in larger, multi-center studies. Second,

while AIUBS demonstrates promise in extracting imaging features, further optimization of automated image analysis algorithms and enhancement of image quality and consistency remain important avenues for technological advancement. Third, future studies could incorporate molecular biomarkers and information on response to molecular-targeted therapies to further refine the model's predictive accuracy and clinical utility.

In conclusion, this study successfully constructed a prediction model for postoperative recurrence and metastasis of breast cancer, integrating clinical features with AIUBS imaging characteristics. By incorporating key risk factors such as lymph node metastasis, tumor staging, AIUBS tumor morphology, and vascularity, the model demonstrated promising predictive ability and stability. Its clinical application may facilitate more individualized management and treatment decisions, potentially leading to improved patient prognosis and quality of life.

Disclosure of conflict of interest

None.

Address correspondence to: Fang Ma, Hefei Second People's Hospital at The Intersection of Guangde Road and Le Lishui Road, Yaohai District, Hefei 230011, Anhui. E-mail: 912869028@qq.com

References

[1] Keresteš V, Kubeš J, Applová L, Kollárová P, Lenčová-Popelová O, Melnikova I, Karabanovich G, Khazeem MM, Bavlovič-Piskáčková H, Štěrbová-Kovaříková P, Austin CA, Roh J, Štěrba M, Šimůnek T and Jirkovská A. Exploring the effects of topoisomerase II inhibitor XK469 on anthracycline cardiotoxicity and DNA damage. Toxicol Sci 2024; 198: 288-302.

[2] Liu C, Li H, Xu K, Song S, He Y, Cai X, Chu X, Yang J and Cui Y. Multiple primary lung cancer versus intrapulmonary metastatic cancer: a case of multiple pulmonary nodules. Thorac Cancer 2019; 10: 352-358.

[3] Claessens AKM, Ibragimova KIE, Geurts SME, Bos MEMM, Erdkamp FLG and Tjan-Heijnen VCG. The role of chemotherapy in treatment of advanced breast cancer: an overview for clinical practice. Crit Rev Oncol Hematol 2020; 153: 102988.

[4] Liang Y, Zhang H, Song X and Yang Q. Metastatic heterogeneity of breast cancer: molecular mechanism and potential therapeutic targets. Semin Cancer Biol 2020; 60: 14-27.

[5] Yang Z, Sun N, Cheng R, Zhao C, Liu J and Tian Z. Hybrid nanoparticles coated with hyaluronic acid lipoid for targeted co-delivery of paclitaxel and curcumin to synergistically eliminate breast cancer stem cells. J Mater Chem B 2017; 5: 6762-6775.

[6] Gu Q, Zhao J, Liu Y, Chen H and Wang L. Association between the systemic immune-inflammation index and the efficacy of neoadjuvant chemotherapy, prognosis in HER2 positive breast cancer-a retrospective cohort study. Gland Surg 2023; 12: 609-618.

[7] Li Y, Wei Y, Tang W, Luo J, Wang M, Lin H, Guo H, Ma Y, Zhang J and Li Q. Association between the degree of fibrosis in fibrotic focus and the unfavorable clinicopathological prognostic features of breast cancer. PeerJ 2019; 7: e8067.

[8] You C, Shen Y, Sun S, Zhou J, Li J, Su G, Michalopoulou E, Peng W, Gu Y, Guo W and Cao H. Artificial intelligence in breast imaging: current situation and clinical challenges. Exploration (Beijing) 2023; 3: 20230007.

[9] Wang J, Chu Y, Wang B and Jiang T. A narrative review of ultrasound technologies for the prediction of neoadjuvant chemotherapy response in breast cancer. Cancer Manag Res 2021; 13: 7885-7895.

[10] Huang X, Qiu Y, Bao F, Wang J, Lin C, Lin Y, Wu J and Yang H. Artificial intelligence breast ultrasound and handheld ultrasound in the BI-RADS categorization of breast lesions: a pilot head to head comparison study in screening program. Front Public Health 2023; 10: 1098639.

[11] Yan LP, Li JY, Tian LL, Wang MY, Yang DW and Xu B. Performance evaluation of artificial intelligence breast ultrasound (AIBUS) in breast cancer screening within primary medical settings. ModernPreventive Medicine 2023; 50: 567-570+576.

[12] Wu GG, Zhou LQ, Xu JW, Wang JY, Wei Q, Deng YB, Cui XW and Dietrich CF. Artificial intelligence in breast ultrasound. World J Radiol 2019; 11: 19-26.

[13] Mahant SS and Varma AR. Artificial intelligence in breast ultrasound: the emerging future of modern medicine. Cureus 2022; 14: e28945.

[14] Wang M, Liu Z and Ma L. Application of artificial intelligence in ultrasound imaging for predicting lymph node metastasis in breast cancer: a meta-analysis. Clin Imaging 2024; 106: 110048.

[15] Dai X, Lu H, Wang X, Liu Y, Zang J, Liu Z, Sun T, Gao F and Sui X. Ultrasound-based artificial intelligence model for prediction of Ki-67 prolif-

eration index in soft tissue tumors. Acad Radiol 2025; 32: 1178-1188.
[16] Tang C, Wang P, Li X, Zhao B, Yang H, Yu H and Li C. Lymph node status have a prognostic impact in breast cancer patients with distant metastasis. PLoS One 2017; 12: e0182953.
[17] Harbeck N and Gnant M. Breast cancer. Lancet 2017; 389: 1134-1150.
[18] Li Z, Wei H, Li S, Wu P and Mao X. The role of progesterone receptors in breast cancer. Drug Des Devel Ther 2022; 16: 305-314.
[19] Ma S, Zhou Y, Ma D, Qi X and Jiang J. Application and challenge of HER2DX genomic assay in HER2+ breast cancer treatment. Am J Cancer Res 2024; 14: 4218-4235.
[20] Harrell FE Jr, Lee KL and Mark DB. Multivariable prognostic models: issues in developing models, evaluating assumptions and adequacy, and measuring and reducing errors. Stat Med 1996; 15: 361-387.
[21] Yerushalmi R, Woods R, Ravdin PM, Hayes MM and Gelmon KA. Ki67 in breast cancer: prognostic and predictive potential. Lancet Oncol 2010; 11: 174-183.
[22] Kundu K, Kuhn T, Kohut A, Staley C, Hanley K and Khanna N. Primary colonic extrauterine endometrial stromal sarcoma: a case and review of the literature. Gynecol Oncol Rep 2020; 32: 100578.
[23] Lin C, Chien SY, Chen LS, Kuo SJ, Chang TW and Chen DR. Triple negative breast carcinoma is a prognostic factor in Taiwanese women. BMC Cancer 2009; 9: 192.
[24] Chen Y, Xie Y, Li B, Shao H, Na Z, Wang Q and Jing H. Automated Breast Ultrasound (ABUS)-based radiomics nomogram: an individualized tool for predicting axillary lymph node tumor burden in patients with early breast cancer. BMC Cancer 2023; 23: 340.
[25] Łuczyńska E, Pawlak M, Popiela T and Rudnicki W. The role of ABUS in the diagnosis of breast cancer. J Ultrason 2022; 22: 76-85.
[26] Giger ML, Inciardi MF, Edwards A, Papaioannou J, Drukker K, Jiang Y, Brem R and Brown JB. Automated breast ultrasound in breast cancer screening of women with dense breasts: reader study of mammography-negative and mammography-positive cancers. AJR Am J Roentgenol 2016; 206: 1341-1350.
[27] Jeh SK, Kim SH, Choi JJ, Jung SS, Choe BJ, Park S and Park MS. Comparison of automated breast ultrasonography to handheld ultrasonography in detecting and diagnosing breast lesions. Acta Radiol 2016; 57: 162-169.
[28] Wang X, Nie L, Zhu Q, Zuo Z, Liu G, Sun Q, Zhai J and Li J. Artificial intelligence assisted ultrasound for the non-invasive prediction of axillary lymph node metastasis in breast cancer. BMC Cancer 2024; 24: 910.
[29] Sun S, Mutasa S, Liu MZ, Nemer J, Sun M, Siddique M, Desperito E, Jambawalikar S and Ha RS. Deep learning prediction of axillary lymph node status using ultrasound images. Comput Biol Med 2022; 143: 105250.
[30] Gu J, Tong T, Xu D, Cheng F, Fang C, He C, Wang J, Wang B, Yang X, Wang K, Tian J and Jiang T. Deep learning radiomics of ultrasonography for comprehensively predicting tumor and axillary lymph node status after neoadjuvant chemotherapy in breast cancer patients: a multicenter study. Cancer 2023; 129: 356-366.
[31] Paduch R. The role of lymphangiogenesis and angiogenesis in tumor metastasis. Cell Oncol (Dordr) 2016; 39: 397-410.